

Spectroscopic Study of Secondary Structure and Thermal Denaturation of Recombinant Human Factor XIII in Aqueous Solution

Aichun Dong,^{*,1} Brent Kendrick,[†] Lotte Kreilgård,[†] James Matsuura,[†] Mark C. Manning,[†] and John F. Carpenter[†]

^{*}Department of Chemistry and Biochemistry, University of Northern Colorado, Greeley, Colorado 80639; and [†]Department of Pharmaceutical Sciences, School of Pharmacy, University of Colorado Health Sciences Center, Denver, Colorado 80262

Received May 23, 1997, and in revised form August 11, 1997

The secondary structure and thermal denaturation (in H₂O vs D₂O) of recombinant human factor XIII in aqueous solutions were investigated using infrared and circular dichroism (CD) spectroscopies. The infrared amide I spectrum of the protein in H₂O solution at 25°C exhibited an absorbance maximum near 1642 cm⁻¹, indicating the presence of a predominantly β -sheet structure. Quantitative analysis revealed that the native protein contains 13–16% α -helix, 41–49% β -sheet, 29% β -turn, and 10–14% extended strand structures. The presence of a strong low-wavenumber β -sheet band at 1641 cm⁻¹ and a weak high-wavenumber β -sheet band at 1689 cm⁻¹ indicated that the β -sheet structure of the protein is predominantly antiparallel. Quantitative analysis of the CD spectrum using the SELCON method indicated a secondary structural content of 10% α -helix, 40–50% β -sheet, 20–35% β -turns, and 20–35% unordered elements, which matches that determined by X-ray crystallography. The apparent discrepancy with the contents of unordered element determined by infrared spectroscopy is reconciled by considering that CD spectroscopy and X-ray crystallography assign extended loops and strands to unordered elements, whereas infrared spectroscopy recognizes these as distinct structured elements. During heating above 60°C, a pair of new infrared bands appeared at 1626 and 1693 cm⁻¹ for the protein in H₂O and 1619 and 1683 cm⁻¹ in D₂O, indicating a formation of intermolecular β -sheet aggregates. The intensities of the new bands increased as a function of temperature, concomitant with an intensity decrease in bands for the native protein structural elements. As expected,

there was an increase in thermal stability in D₂O relative to that in H₂O, which was manifested as an increase of about 5°C in the temperature for initial loss of infrared bands assigned to native structural elements and for appearance of bands due to intermolecular β -sheet. In addition, the midpoint of the thermally induced transitions in infrared spectra were about 2.5°C higher in D₂O than in H₂O. Based on the infrared analysis, the thermally denatured state of the protein in both H₂O and D₂O contains predominantly intermolecular β -sheet. The broad, poorly resolved absorbance that spans the region between the intermolecular β -sheet bands was assigned to an ensemble of heterogeneous structural elements (including unordered), none of which is populated to a high enough degree to result in a distinct infrared band. Results from CD spectroscopy support these conclusions about the structure of the denatured, aggregated protein. © 1997 Academic Press

Factor XIII (FXIII),² a transglutaminase (protein-glutamine:amine γ -glutamyltransferase, EC 2.3.2.13), is a zymogen important in the coagulation process. The active enzyme catalyzes covalent cross-linking between fibrin molecules (1, 2) and of fibrin to fibronectin and thrombospondin (3, 4), which stabilizes the blood clot and attaches it to the site of injury, respectively. The protein exists as two forms, a tetramer from plasma and a homodimer found in platelets and the placenta (5). The homodimeric form, the subject of the current study, has been expressed to high yield in yeast and purified (6), and the protein's structure and thermal

¹ To whom correspondence should be addressed. Fax: (970) 351-1269.

² Abbreviations used: rFXIII, recombinant factor XIII; FT-IR, Fourier transform infrared; CD, circular dichroism.

stability have been well characterized (7, 8). The two subunits are noncovalently associated (9). The X-ray crystal structure, resolved to 2.8 Å, shows that each chain of the protein is folded into four sequential structural regions: β -sandwich, core, β -barrel 1, and β -barrel 2 (7). The core is a mix of α -helix and β -sheet and the secondary structures of the other three domains is predominantly antiparallel β -sheet (7). Thermal denaturation studies with fluorescence spectroscopy and differential scanning calorimetry documented that each subunit consists of three thermally labile domains and two extremely thermally stable domains (8). Of greatest interest for the current study is the observation that the thermal denaturation of the labile domains, at near neutral pH, is irreversible because of the formation of protein aggregates (8).

This background of structural and thermal stability data makes recombinant Factor XIII (rFXIII) an excellent model protein for the purpose of the current study, which was to use infrared and circular dichroism (CD) spectroscopies to determine the secondary structure of the protein in solution and to compare thermally induced structural transitions and stability in H₂O- and D₂O-based buffers. Infrared (10–14) and CD (15–17) spectroscopies have been used extensively in studies of secondary structural composition of proteins. Moreover, infrared spectroscopy has been used to study thermal denaturation and aggregation of several proteins (18). However, in all cases, except a study on ribonuclease A (19), these transitions have only been analyzed for proteins prepared in D₂O. It has long been known that deuteration increases the thermal stability of proteins (20, 21). Therefore, it was of interest to compare thermally induced structural transitions in the two solvents by Fourier transform infrared (FT-IR) spectroscopy. Finally, since we found that the thermally induced protein aggregates (formed at pH 8.0) were optically transparent, we were also able to use CD spectroscopy to corroborate the infrared spectroscopic assessment of the structure of the final thermally denatured/aggregated state of the protein.

MATERIALS AND METHODS

Protein preparation. Recombinant human Factor XIII expressed in *Saccharomyces cerevisiae* (6) was generous gift from ZymoGenetics, Inc. (Seattle, WA). For the H₂O solution, the lyophilized protein was dissolved in 10 mM Tris–HCl buffer, pH 8.0, containing 0.1 mM EDTA at concentration of 20 mg/mL and dialyzed against same buffer at 4°C overnight to remove stabilizing additives (i.e., sucrose and glycine) present in the lyophilized formulation. For D₂O solution, the protein was first dissolved in 10 mM Tris–HCl/H₂O buffer, pH 8.0, containing 0.1 mM EDTA and dialyzed against same buffer to remove stabilizing additives. After dialysis the protein solution was mixed with D₂O (99.9 at.% D, Sigma) at 1:2 ratio and lyophilized using a Labconco 4.5 freeze drier. The sample was then rehydrated in 10 mM Tris–HCl/D₂O, pD 7.9, at a concentration of 20 mg/mL.

Infrared spectroscopy. Infrared spectra of rFXIII were measured with a Magna-IR 550 spectrometer (Nicolet) equipped with a dTGS

detector. Protein samples, both in H₂O and D₂O, were prepared in a heatable cell (P/N 20500, Graseby) with CaF₂ windows and a 6- μ m spacer. For each spectrum, a 256-scan interferogram was collected in a single beam mode with a 4 cm⁻¹ resolution. Reference spectra were recorded as 256-scan interferogram under identical scan conditions with only the corresponding buffer in the cell. Protein spectra were obtained according to previously established criteria and double-subtraction procedure (12, 22). The resultant spectra were smoothed with a 7-point Savitsky–Golay smooth function to remove the white noise. Second-derivative spectra were obtained by the derivative function of Omnic software (Nicolet). The inverted second-derivative spectra were obtained by factoring by -1 and then baseline corrected as previously described (18). Fourier self-deconvolution was carried out using a half-bandwidth (full-width at half-height) of 25 cm⁻¹ and an enhance factor (*K* value) of 2.7. Curve-fitting to second-derivative and Fourier self-deconvoluted spectra was performed as previously described (23, 24). For the thermal denaturation experiments, the chosen temperature at which a spectrum was acquired was controlled within 0.3°C using a custom-built Peltier cell temperature controller. Spectral acquisition at a given temperature required approximately 5 min (i.e., dwell time at the given temperature). The average heating rate between spectral acquisition temperatures was about 0.5°C/min.

Circular dichroism spectroscopy. The far-UV CD spectra were recorded with an Aviv Model 62DS spectrometer (Lakewood, NJ) in the wavelength range of 185–260 nm using a pathlength of 10 μ m. Spectra were background corrected and converted to mean residue ellipticity (deg cm²/dmol). CD spectra (185–260 nm) were deconvoluted using SELCON, as previously described (25). Spectral acquisition at a given temperature required approximately 20 min and the heating rate between these temperatures was about 1.5°C/min.

Determination of midpoint of thermal transitions. The plots of the transitions in infrared spectroscopic absorbances as a function of temperature were fitted with a sigmoidal function (SigmaPlot). The inflection point in the plot was taken as the midpoint of the transition.

RESULTS

Infrared spectra of rFXIII. Figure 1 shows the infrared spectra of rFXIII (20 mg/mL) in H₂O solution recorded at various temperatures. At temperatures below 55°C, the spectra of rFXIII in the conformationally sensitive amide I region, which is due predominantly to the C = O stretching vibration of the protein backbone, have absorbance maxima at 1642 cm⁻¹, indicating a predominantly β -sheet structure (10, 12, 22, 26). This result is consistent with those reported by X-ray crystallographic analysis (7). As temperature increased to above 55°C, the amide I absorbance maxima were red-shifted about 14 cm⁻¹ to near 1628 cm⁻¹, indicating the formation of intermolecular β -sheet aggregate (18, 27–30). After cooling the sample from 75 back to 25°C, the amide I absorbance maximum shifted about 2 cm⁻¹ further to a lower wavenumber near 1626 cm⁻¹, indicating an irreversible thermal denaturation and the retention of protein aggregates. The thermally induced spectral changes in the amide I region were accompanied by similar changes in the amide II region, which arise mainly from an out-of-phase combination of N–H in-plane bending and C–N stretching vibrations of peptide linkages (31).

To characterize the secondary structure of rFXIII

in its native state, two independent mathematical band-narrowing procedures, namely Fourier self-deconvolution and calculation of the second-derivative, together with curve-fitting analysis were carried out. Figure 2 shows the curve-fitted Fourier self-deconvolution and inverted second-derivative spectra of rFXIII at 25°C. Both methods revealed amide I band components ascribed to extended strands (1628 cm^{-1}), β -sheet (1689 and 1641 cm^{-1}), α -helix (1655 cm^{-1}), and β -turn (1661, 1674, and 1680 cm^{-1}) structures (22, 32). The concomitant appearance of a strong low-wavenumber β -sheet band at 1641 cm^{-1} and a weak high-wavenumber β -sheet band at 1689 cm^{-1} suggests that rFXIII contains predominantly antiparallel β -sheet structure (10, 31, 33). This result is consistent with the X-ray crystallographic analysis of the protein (7). Quantitative analysis of the amide I spectra revealed that rFXIII contains 13–16% α -helix, 41–49% β -sheet, 29% β -turn, and 10–14% extended structures (Table I). To further analyze the effects of heating on rFXIII's structure in H_2O , Fig. 3A presents an overlay of the second-derivative spectra of rFXIII in the amide I region, which were generated from spectra acquired during heating. At temperatures between 25 and 55°C, the secondary structure of rFXIII remains relatively unchanged. As temperature increased to 60°C and above, an intensity decrease in the 1641, 1655, 1674, and 1689 cm^{-1} bands, accompanied by an intensity increase in the 1626 and 1693 cm^{-1} bands, was observed. These thermally induced spectral changes suggest a major structural transition from native α -helix, turn, and

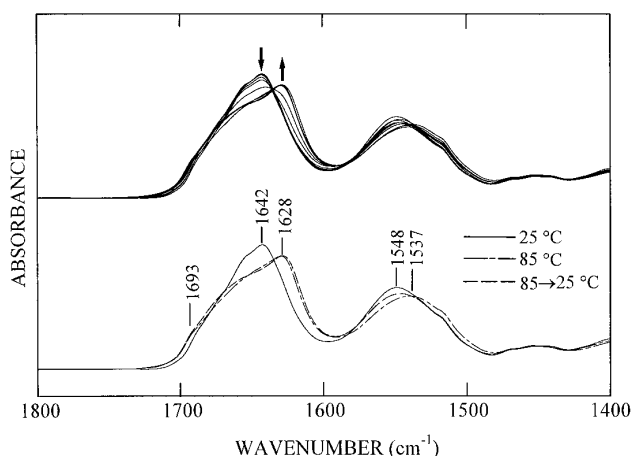


FIG. 1. Infrared spectra of rFXIII in 10 mM Tris-HCl/0.1 mM EDTA (pH 8.0) recorded at various temperatures. (Top curve) The spectra of rFXIII at 25, 35, 45, 55, 60, 65, 70, 75, and 85°C. Arrows represent the direction of intensity changes as temperature increases. (Bottom curve) The spectra of rFXIII at 25, 85, and at 25°C after cooled from 85°C. The spectral contributions of the liquid and gaseous water have been subtracted as described under Materials and Methods.

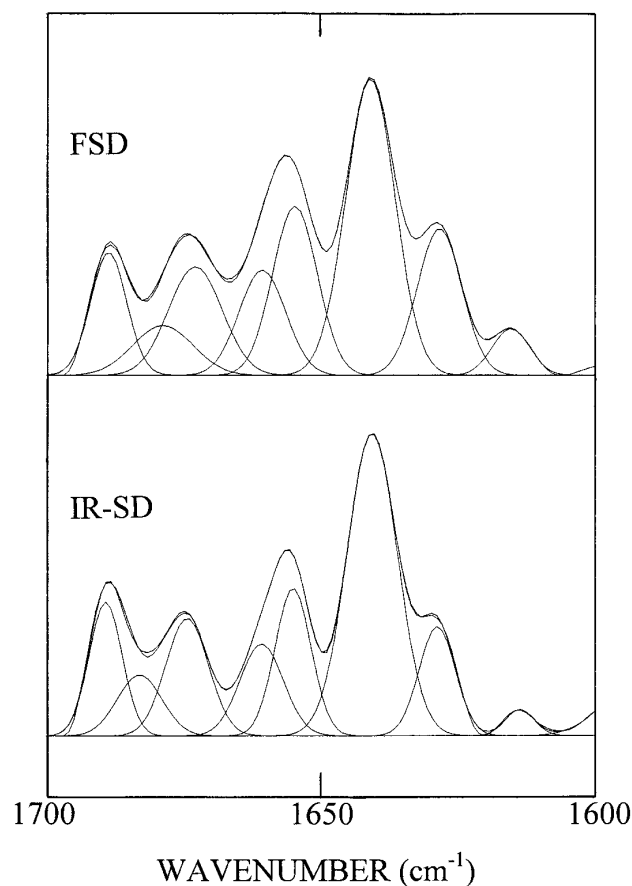


FIG. 2. The curve-fitting analysis of infrared spectra of native rFXIII at 25°C. (Top) The curve-fitted Fourier self-deconvoluted spectrum. (Bottom) The curve-fitted inverted second-derivative spectrum. Detailed parameters are listed in Table I.

intramolecular β -sheet to intermolecular β -sheet aggregates (27–30, 34, 35). At 75–85°C, intermolecular β -sheet accounts for about 48% of total secondary structure. Interestingly, there was not a new band observed near $1648 \pm 2 \text{ cm}^{-1}$, a region assigned to unordered (random coil) elements (12, 22), during thermal denaturation. The assignment of amide I components at $1648 \pm 2 \text{ cm}^{-1}$ to unordered structure for proteins in H_2O solution was made from the empirical studies of more than 60 different proteins (Protein Infrared Database;³ 12, 19, 22). The lack of a major contribution from a band component near 1648 cm^{-1} can be interpreted reasonably to the lack of a substantial amount of unordered elements in the denatured state. The spectrum recorded at 25°C, after cooling from 85°C, exhibits a similar spectral pattern as the spectrum recorded at 85°C with the exception of a 2 cm^{-1} red shift of the strong low-wave-

³ Protein Infrared Database by Dong, A., Carpenter, J. F., and Caughey, W. S. (<http://www.univnorthco.edu/chemist/aichun/irdata.htm>).

TABLE I

Relative Areas and Assignments of Deconvoluted Infrared Amide I Band Components of Recombinant Human Factor XIII in H₂O at 25°C

Frequency (cm ⁻¹)	Relative area (%) ^a		Assignment
	IR-SD ^b	FSD/CF ^c	
1628	9.8	14.1	Extended strand
1641	37.5	31.2	β -Sheet
1655	13.0	16.0	α -Helix
1661	9.7	10.4	Turn
1674	12.3	12.4	Turn
1680	6.7	6.5	Turn
1689	11.0	9.4	β -Sheet

^a Area of the band near 1614 cm⁻¹ assignable to side chain vibration is not included in calculation.

^b Infrared second-derivative, the method of Dong *et al.* (23).

^c Fourier self-deconvolution/curve-fitting, the method of Susi and Byler (10).

number β -sheet band (Fig. 3B). Thus, the process of thermal denaturation and aggregation of rFXIII at pH 8.0 is irreversible, which is consistent with earlier fluorescent spectroscopic and differential scanning calorimetric results (8).

To determine whether the solvent system used affected the thermal denaturation process, we also examined the thermal denaturation of rFXIII in D₂O solution. Figure 4A shows an overlay of second-derivative spectra of rFXIII (20 mg/mL) in D₂O solution at various temperatures. The amide I band assignments for rFXIII in D₂O are made on the basis of earlier studies of other proteins in this solvent (10, 11, 26, 32). For the spectrum of the native state at 25°C, the bands near 1685 and 1638 cm⁻¹ can be assigned to β -sheet; the band near 1653 cm⁻¹ to α -helix; the band near 1668 cm⁻¹ to turns; and the shoulder at 1628 cm⁻¹ to extended strands. As temperature increased, an intensity decrease at the 1639 cm⁻¹ band (native β -sheet structure), concomitant with an intensity increase at the 1619 cm⁻¹ band (intermolecular β -sheet aggregate), was observed. It is noteworthy that both the native and the thermally denatured states exhibited a high-wavenumber β -sheet band near 1683 cm⁻¹, which in the native protein can be assigned to intramolecular antiparallel β -sheet and in the denatured state to intermolecular β -sheet of protein aggregates. At temperature above 70°C, the bands at 1619 and 1683 cm⁻¹ become dominant features of the spectra. The remaining components fused together and became a broad band centered near 1645 cm⁻¹. The spectrum recorded at 25°C, after cooling from 85°C, exhibits a similar spectral pattern as the spectra recorded at 85°C with the exception of a 2 cm⁻¹ red shift of the strong low-wavenumber β -sheet band (Fig. 4B). Thus, as in H₂O, thermal denaturation and aggregation of the protein in D₂O is irreversible.

The close correlations between the formation of intermolecular β -sheet aggregates and the disappearance of the native β -sheet structure in rFXIII in both H₂O and D₂O solutions during the course of thermal denaturation are shown in Fig. 5 as plots of the intensity values for bands at 1641 and 1626 cm⁻¹ in H₂O and at 1638 and 1619 cm⁻¹ in D₂O as a function of temperature. The overall thermally induced changes were very similar in both solvents. In both cases, a native β -sheet structure was converted to an intermolecular β -sheet aggregate. However, the protein was considerably more stable in D₂O than in H₂O. The onsets for the thermally induced transitions are between 55 and 60°C in H₂O and between 60 and 65°C in D₂O. The midpoints of the transitions are 62.9 and 65.4°C, respectively, in H₂O and D₂O.

Circular dichroism spectra of rFXIII. CD spectra of rFXIII were measured in order to verify the secondary structural composition and thermal behavior of the protein. Unlike infrared spectra, CD spectra are unaf-

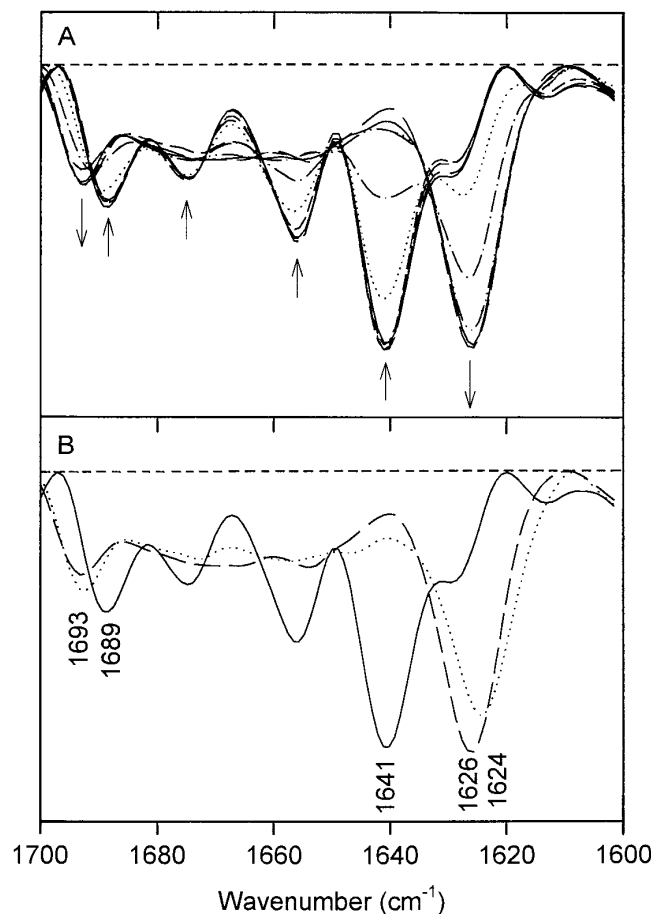


FIG. 3. The second-derivative infrared spectra of rFXIII in H₂O at various temperatures. (A) The spectra of rFXIII at 25, 35, 45, 55, 60, 65, 70, 75, and 85°C. Arrows represent the direction of intensity changes as temperature increase. (B) The spectra of rFXIII at 25°C (—), 85°C (---), and at 25°C after cooling from 85°C (⋯⋯⋯).

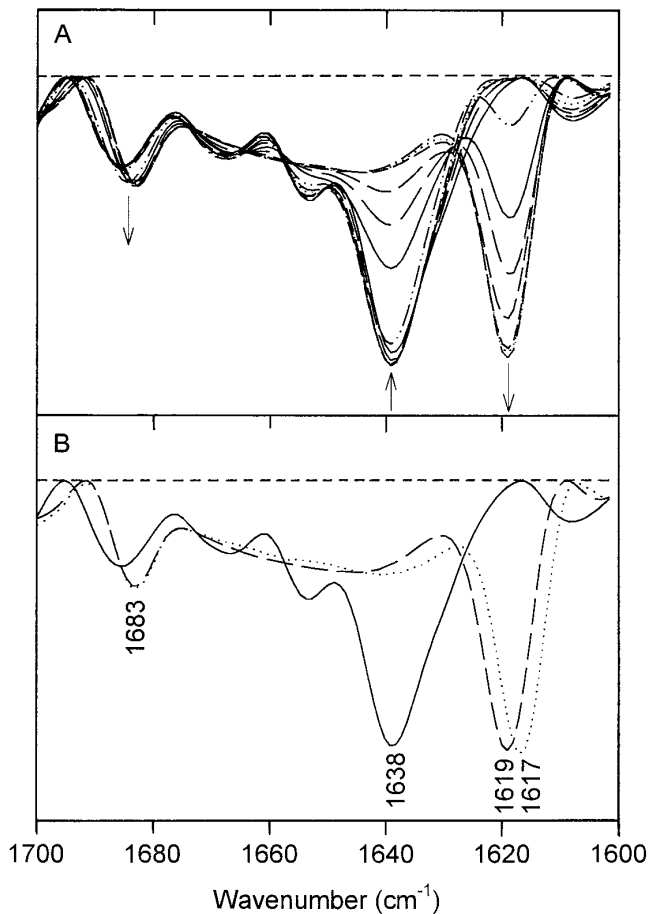


FIG. 4. The second-derivative infrared spectra of rFXIII in D_2O at various temperatures. (A) The spectra of rFXIII at 25, 35, 45, 50, 55, 60, 65, 65.5, 66, 70, 75, 80, and 85°C. Arrows represent the direction of intensity changes as temperature increase. (B) The spectra of rFXIII at 25°C (—), 85°C (---), and at 25°C after cooled from 85°C (·····).

ected by deuteration of the protein (24). At 25°C, rFXIII displays a far-UV CD spectrum with a single negative maximum at 211 nm and a positive band near 196 nm (Fig. 6). This type of pattern is consistent with a protein having a large β -sheet content along with small amounts of α -helix (36). Quantitative analysis of the spectrum using the SELCON method of Sreerama and Woody (25) indicated a secondary structural content of 10% α -helix, 40–50% β -sheet, 20–35% β -turns, and 20–35% random or unordered elements.

During thermal denaturation of 20 mg/mL protein in H_2O buffer, as the temperature increased, the negative band shifted to 217 nm and became more intense (Fig. 6). A negative band at 217 nm is consistent with a structure composed almost entirely of β -sheet (17, 37) and supports the infrared spectroscopic measurements indicating increased intermolecular β -sheet formation. Upon cooling from 70°C back to 25°C, the spectrum

does not revert, but is similar to that found at elevated temperature, indicating that the denaturation and aggregation were irreversible.

Finally, as seen with infrared spectroscopy (Fig. 7), the CD spectra of the thermally denatured protein in H_2O and D_2O had only minor differences (Fig. 8). The negative band near 217 nm is broadened and more intense in H_2O than in D_2O . Furthermore the crossover is blue-shifted in H_2O relative to that seen in D_2O . More importantly, the intense negative band at 217 nm is consistent with structures composed largely of β -sheet (17, 37) and supports the infrared spectroscopic determination of a predominantly intermolecular β -sheet content of the denatured protein in both solvents.

DISCUSSION

Secondary structure of native rFXIII. Both infrared and CD spectroscopies indicated that the secondary structure of native rFXIII in H_2O is predominantly β -

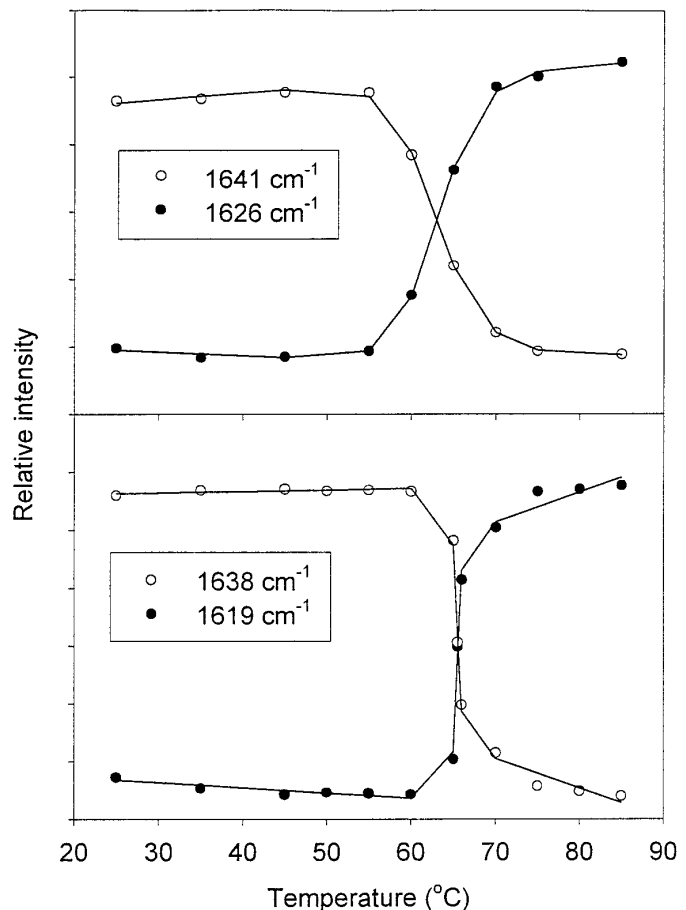


FIG. 5. Temperature-dependent intensity changes of the amide I components assigned to the native β -sheet structure and intermolecular β -sheet aggregates. (Top) rFXIII in H_2O . (Bottom) rFXIII in D_2O .

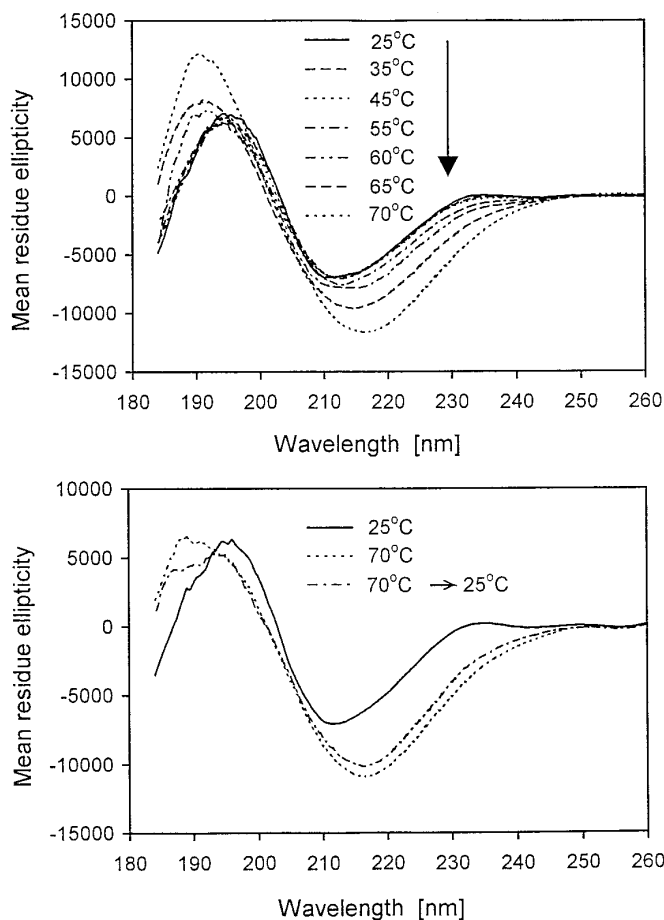


FIG. 6. The far-UV CD spectra of rFXIII in H₂O recorded at various temperatures. (Top) The spectra of rFXIII at during heating from 25 to 70°C. (Bottom) The spectra of rFXIII at 25, 70, and at 25°C after cooled from 70°C.

sheet, which agrees well with the structure determined by X-ray crystallography (7). However, there are some apparent discrepancies in the percentages of secondary structural types determined by FT-IR spectroscopy relative to those seen with X-ray crystallography and CD spectroscopy. Deconvolution of the CD spectrum using SELCON (25) shows that rFXIII contains approximately 10% α -helix, 40–50% β -sheet, 20–35% β -turns, and 20–35% random or unordered elements. These values agree well with those determined by X-ray crystallography (7, 38). In contrast, the infrared spectroscopic data (Table I) indicates that there is about 13–16% α -helix, 41–49% β -sheet, 29% β -turn, and 10–14% extended structures. There is no indication of random or unordered elements, because there is not an infrared component in the region of $1648 \pm 2 \text{ cm}^{-1}$, which is usually assigned to such elements (12, 22).

Thus, the major discrepancy is the apparent lack of random or unordered components in the secondary structure as determined by FT-IR spectroscopy. This

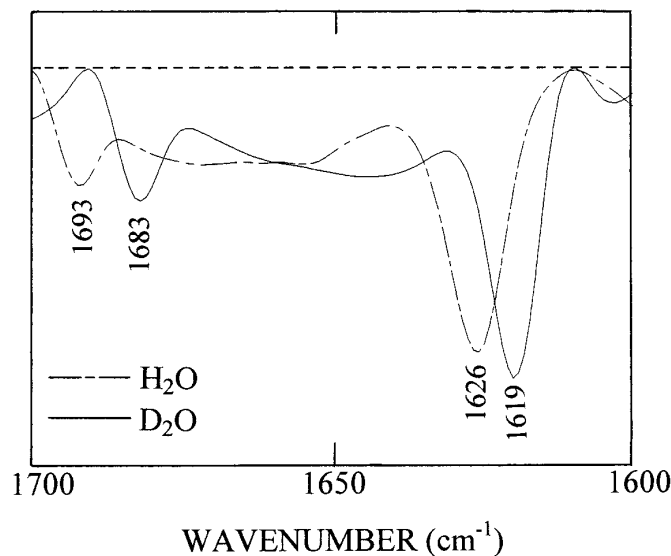


FIG. 7. Comparison of the second-derivative spectra of thermally denatured state of rFXIII in H₂O and D₂O at 85°C.

issue can be resolved by considering how the three methods assign structural definition to a given structural element. First, it is unusual that CD spectroscopy finds such a high proportion of so-called random structure. Its presence is suggested by the low relative intensity of the 195-nm positive band (Fig. 6), which is greatly reduced relative to the negative band at 213 nm. These spectral features indicate that a strong negative component must occur near 200 nm. The bathochromic shift of the negative band from the canonical value of 217 nm for β -sheets (17) further supports this argument. Second, with X-ray crystal structures the regions assigned to random or unordered elements are those that do not meet the criteria for assignment for

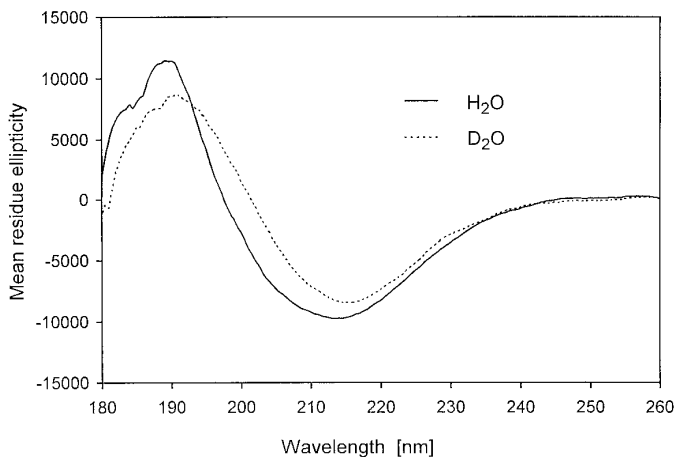


FIG. 8. Far-UV CD spectra at 80°C of rFXIII thermally denatured in H₂O and D₂O.

helices, β -sheets, or turns (cf. 39). In particular, turns are assigned to residues that are not part of the α -helix or β -sheet assignments and for which the C^α backbone bends sharply at each of these residues (α_1 in the range -90° to 90°). Visual examination of the X-ray crystal structure reveals several extended strands and large loop regions bridging helices and sheets, which would not be recognized as turns based on these criteria, and, thus, assigned to unordered elements (7). Apparently, CD spectroscopy also recognizes these structures as being unordered.

In contrast, these extended strands and loops do not give rise to a distinct band for random or unordered elements in the infrared spectrum. There are two features in the infrared spectrum that could account for this observation. First, in addition to the two prominent β -sheet bands at 1641 and 1689 cm^{-1} , there is a weaker feature at 1628 cm^{-1} , which is still within the frequency range usually attributed to β -sheet (Fig. 3). This band can be assigned to the extended strands (32) and accounts for about 10–14% of the secondary structure, which is consistent with the X-ray crystal structure (7). Second, there is a spectral feature at 1661 cm^{-1} accounting for about 10% of the secondary structure (Fig. 3; Table I), which is typically assigned to 3_{10} -helix or Type III turn structures (22). The X-ray crystal structure does not display any significant amount of 3_{10} -helix, suggesting that the band at 1661 cm^{-1} is due to loops or distorted turns. This would not be surprising, because often bands in the 1660–1685 cm^{-1} are assigned to turns. Thus, given these infrared band assignments and the apparent assignment of loops and extended strands to unordered elements by CD spectroscopy and X-ray crystallography, the secondary structural compositions given by three methods are very similar.

Thermal denaturation of rFXIII. Many previous studies have found that thermal denaturation of proteins occurs at temperatures several degrees higher in D_2O than in H_2O (20, 21). It has been known for decades that hydrogen bonds involving deuterium are stronger than those formed by hydrogen (40, 41). By exchanging the protons of polypeptide and protein backbones to deuterons, the hydrogen bonding strength in the macromolecule is significantly increased, which, in turn, increases the conformational stability of polypeptides and proteins (21, 22, 42). With rFXIII, the increase in stability in D_2O relative to that in H_2O was manifested as an increase of about 5°C in the temperature for initial loss of infrared bands assigned to native structural elements and for appearance of bands due to intermolecular β -sheet (Fig. 5). In addition, the midpoint of the thermally induced transitions in infrared spectra were about 2.5°C higher in D_2O than in H_2O .

However, the overall structural transitions detected

by FT-IR spectroscopy during thermal unfolding and subsequent aggregation were very similar in H_2O and D_2O (Figs. 3 and 4). In both solvents, heating induces an irreversible loss of bands ascribed to native α -helix, β -sheet, and turn structures, which can be attributed to unfolding of the thermal labile regions in the N-terminal β -sandwich and the molecular core (7, 8). There is also a concomitant irreversible increase in the absorbance of bands due to intermolecular β -sheet in protein aggregates. These transitions are similar to those noted in previous studies of thermal denaturation of numerous proteins, which have structures ranging from predominantly α -helix to predominantly β -sheet, in D_2O (18, 27–30, 34, 35). In these studies, the spectra for thermally denatured proteins were characterized by a strong low-wavenumber β -sheet band between 1628 and 1615 cm^{-1} and a weak high-wavenumber β -sheet band between 1695 and 1680 cm^{-1} , which were due to intermolecular β -sheet in protein aggregates.

Also, the intervening spectral region was characterized by a single broad absorbance centered around 1645 cm^{-1} in D_2O , which has been attributed to random coil (27–30, 34, 35). With rFXIII, in both H_2O and D_2O , we also found that a single, broad absorbance separates the prominent intermolecular β -sheet bands (Fig. 7). The broad absorbance spans the spectral range from about 1640 to 1685 cm^{-1} in H_2O and from 1630 to 1675 cm^{-1} in D_2O and encompasses regions usually assigned to β -sheet, random, α -helix, and turn structures. There are not any apparent, clearly resolved bands in this region. The lack of resolution is further emphasized by the finding that in this region of the fourth-derivative spectra (data not shown) no distinct bands were resolved in the spectrum of the sample denatured in D_2O and only a weak band for α -helix at about 1655 cm^{-1} in the spectrum for the sample denatured in H_2O was resolved. Similarly, the CD spectra of the thermally denatured proteins in both solvents are indicative of high β -sheet contents (Fig. 8). However, there are spectral differences worth noting. In the CD spectrum for the H_2O sample, the negative band is more intense and broadened than that seen in the spectrum for the D_2O sample. Furthermore, the cross-over wavelength is blue-shifted in the CD spectrum of the H_2O sample and the 192-nm positive band is more intense and sharp than that seen in the CD spectrum of the D_2O sample. These differences indicate that in the H_2O sample, unlike the D_2O sample, there is some helical structure present, consistent with the FT-IR spectroscopic results.

Based on our infrared and CD spectroscopic results, we assign the broad relatively undefined absorbance in the center of the infrared amide I spectra of the thermally denatured protein to an ensemble of poorly defined structural elements (cf. 30), none of which is pop-

ulated to high enough degree to result in a distinct absorbance band in the second derivative spectra (Fig. 7). Clearly among these elements would be some fraction that could be considered as unordered or random, but also a highly heterogeneous mixture of helix, coil, and turn structures. In conclusion, conducting the thermal denaturation of rFXIII in either H₂O or D₂O results in similar final structures in which only the intermolecular β -sheet elements are clearly defined.

ACKNOWLEDGMENTS

We gratefully acknowledge ZymoGenetics for the gift of recombinant human Factor XIII. We thank Prof. David C. Teller for providing us with estimates of the protein's secondary structural composition based on the X-ray crystallography data. This work was supported in part by National Science Foundation Grant BES9505301 to J.F.C., University of Northern Colorado Research Corporation to A.D., and predoctoral fellowships to B.K. from the American Foundation for Pharmaceutical Education and the Colorado Institute for Research in Biotechnology.

REFERENCES

- Folk, J. E. (1980) *Annu. Rev. Biochem.* **49**, 517–531.
- McDonagh, J. A. (1987) in *Hemostasis and Thrombosis* (Colman, R. W., Hirsh, J., Marder, V., and Salzman, E. W., Eds.), pp. 289–300, Lippincott, Philadelphia.
- Hansen, M. S. (1984) *Thromb. Res.* **34**, 551–556.
- Bale, M. D., and Mosher, D. F. (1986) *Biochemistry* **25**, 5667–5673.
- Henschen, A., and McDonagh, J. (1986) in *Blood Coagulation* (Zwally, R. F. A., and Hemker, J. C., Eds.), pp. 171–241, Elsevier, Amsterdam.
- Bishop, P. D., Teller, D. C., Smith, R. A., Lasser, G. W., Gilbert, T., and Seale, R. L. (1990) *Biochemistry* **29**, 1861–1869.
- Yee, V. C., Pedersen, L. C., Trong, I. L., Bishop, P. D., Stenkamp, R. E., and Teller, D. C. (1994) *Proc. Natl. Acad. Sci. USA* **91**, 7296–7300.
- Kurochkin, I. V., Procyk, R., Bishop, P. D., Yee, V. C., Teller, D. C., Ingham, K. C., and Medved, L. V. (1995) *J. Mol. Biol.* **248**, 414–430.
- Ichinose, A., Hendrickson, L. E., Fujikawa, K., and Davie, E. W. (1986) *Biochemistry* **25**, 6900–6906.
- Susi, H., and Byler, D. M. (1986) *Methods Enzymol.* **130**, 290–311.
- Surewicz, W. K., and Mantsch, H. H. (1988) *Biochim. Biophys. Acta.* **952**, 115–130.
- Dong, A., Huang, P., and Caughey, W. S. (1990) *Biochemistry* **29**, 3303–3308.
- Arrondo, J. L., Muga, A., Castresana, J., and Goni, F. M. (1993) *Prog. Biophys. Mol. Biol.* **59**, 23–56.
- Surewicz, W. K., Mantsch, H. H., and Chapman, D. (1993) *Biochemistry* **32**, 389–394.
- Hennessey, J. P., Jr., and Johnson, C., Jr. (1981) *Biochemistry* **20**, 1085–1094.
- Manning, M. C. (1992) in *Biocatalyst Design for Stability and Specificity* (Himmel, M. E., and Georgiou, G., Eds.), ACS Symposium Series, 516, pp. 33–52.
- Towell, J. F., III, and Manning, M. C. (1994) in *Analytic Applications of Circular Dichroism* (Purdie, N., and Brittain, H. G., Eds.), pp. 175–205, Elsevier, New York.
- Dong, A., Prestrelski, S. J., Allison, S. D., and Carpenter, J. F. (1995) *J. Pharm. Sci.* **84**, 415–424.
- Yamamoto, T., and Tasumi, M. (1991) *J. Mol. Struct.* **242**, 235–244.
- Hermans, J., Jr., and Scheraga, H. A. (1959) *Biochim. Biophys. Acta* **36**, 534–535.
- Scheraga, H. A. (1960) *Ann. NY Acad. Sci.* **84**, 608–616.
- Dong, A., and Caughey, W. S. (1994) *Methods Enzymol.* **232**, 139–175.
- Dong, A., Caughey, B., Caughey, W. S., Bhat, K. S., and Coe, J. E. (1992) *Biochemistry* **31**, 9364–9370.
- Dong, A., Matsuura, J., Allison, S. D., Chrisman, E., Manning, M. C., and Carpenter, J. F. (1996) *Biochemistry* **35**, 1450–1457.
- Sreerama, N., and Woody, R. W. (1993) *Anal. Biochem.* **209**, 32–44.
- Byler, D. M., and Susi, H. (1986) *Biopolymers* **25**, 469–487.
- Clark, A. H., Saunderson, D. P. H., and Suggett, A. (1981) *Int. J. Pept. Protein Res.* **17**, 353–364.
- Casal, H. L., Köhler, U., and Mantsch, H. H. (1988) *Biochim. Biophys. Acta.* **957**, 11–20.
- Byler, D. M., and Purcell, J. M. (1989) *SPIE Fourier Transform Spectrosc.* **1145**, 415–417.
- Ismail, A. A., Mantsch, H. H., and Wong, P. T. T. (1992) *Biochim. Biophys. Acta* **1121**, 183–188.
- Krimm, S., and Bandekar, J. (1986) *Adv. Protein Chem.* **38**, 181–364.
- Prestrelski, S. J., Byler, D. M., and Liebman, M. M. (1992) *Proteins: Struct. Func. Gen.* **14**, 440–450.
- Chirgadze, Y. N., and Nevskaya, N. A. (1976) *Biopolymers* **15**, 607–625.
- Muga, A., Mantsch, H. H., and Surewicz, W. K. (1991) *Biochemistry* **30**, 7219–7224.
- Surewicz, W. K., and Olesen, P. R. (1995) *Biochemistry* **34**, 9655–9660.
- Manning, M. C., and Woody, R. W. (1991) *Biopolymers* **31**, 569–586.
- Matsuura, J., and Manning, M. C. (1994) *J. Agric. Food Chem.* **42**, 1650–1656.
- Teller, D. C. (1996) personal communication.
- Levitt, M., and Greer, J. (1977) *J. Mol. Biol.* **114**, 181–239.
- Calvin, M., Hermans, J., Jr., and Scheraga, H. A. (1959) *J. Am. Chem. Soc.* **81**, 5048–5050.
- Tomita, K.-I., Rich, A., De Loze, C., and Blout, E. R. (1962) *J. Mol. Biol.* **4**, 83–92.
- Maybury, R. H., and Katz, J. J. (1956) *Nature* **177**, 629–631.